

Systems biology approach to exploring the effect of cyclic stretching on cardiac cell physiology

Chien-Cheng Chen^{1,*}, Tzyy-Yue Wong^{2,*}, Tzu-Yun Chin³, Wen-Hsien Lee^{4,5,6}, Chan-Yen Kuo⁷, Yi-Chiung Hsu³

¹Department of Cardiology, Show Chwan Memorial Hospital, Changhua, Taiwan

²International Center for Wound Repair and Regeneration National Cheng Kung University, Tainan, Taiwan

³Department of Biomedical Sciences and Engineering, National Central University, Taoyuan, Taiwan

⁴Graduate Institute of Clinical Medicine, College of Medicine, Kaohsiung Medical University, Kaohsiung, Taiwan

⁵Department of Internal Medicine, Kaohsiung Municipal Hsiao-Kang Hospital, Kaohsiung Medical University, Kaohsiung, Taiwan

⁶Department of Internal Medicine, School of Medicine, College of Medicine, Kaohsiung Medical University, Kaohsiung, Taiwan

⁷Department of Research, Taipei Tzu Chi Hospital, Buddhist Tzu Chi Medical Foundation, New Taipei, Taiwan

*Equal contribution

Correspondence to: Chan-Yen Kuo, Yi-Chiung Hsu; email: cykuo863135@gmail.com, syicncu@g.ncu.edu.tw

Keywords: next-generation sequencing, cyclic stretching, cardiac cell, functional enrichment

Received: March 11, 2020

Accepted: May 27, 2020

Published: August 5, 2020

Copyright: Chen et al. This is an open-access article distributed under the terms of the Creative Commons Attribution License (CC BY 3.0), which permits unrestricted use, distribution, and reproduction in any medium, provided the original author and source are credited.

ABSTRACT

Although mechanical forces are involved in pressure-overloaded cardiomyopathy, their effects on gene transcription profiles are not fully understood. Here, we used next-generation sequencing (NGS) to investigate changes in genomic profiles after cyclic mechanical stretching of human cardiomyocytes. We found that 85, 87, 32, 29, and 28 genes were differentially expressed after 1, 4, 12, 24, and 48 hours of stretching. Furthermore, 10 of the 29 genes that were up-regulated and 11 of the 28 that were down-regulated after 24 h showed the same changes after 48 h. We then examined expression of the genes that encode serpin family E member 1 (SERPINE1), DNA-binding protein inhibitor 1 (ID1), DNA-binding protein inhibitor 3 (ID3), and CCL2, a cytokine that acts as chemotactic factor in monocytes, in an RT-PCR experiment. The same changes were observed for all four genes after all cyclic stretching durations, confirming the NGS results. Taken together, these findings suggest that cyclical stretching can alter cardiac cell physiology by activating cardiac cell metabolism and impacting cholesterol biosynthesis signaling.

INTRODUCTION

Mechanical stretching affects many cellular functions, including proliferation, differentiation, and survival [1, 2]. Furthermore, cyclic stretching promotes differentiation, survival, and migration in mesenchymal stem cells [3, 4]. Bin Fang et al. showed that cyclic stretch promoted survival, proliferation, adhesion, and migration, while prolonged stretching promoted aging, in adipose-derived stem cells (ADSCs) [5]. Other

mechanical stimuli, including shear forces, tissue stiffness, and tissue stretch, affected stem cell fate and differentiation of human-induced pluripotent stem cells (hiPSCs) into cardiomyocytes [6–8]. Furthermore, *in vitro* cyclic stretching enhanced the growth of adult stem cells, human pluripotent cells, and cardiomyocytes by regulating cell contractility and sarcomere maturation [9]. However, increased stretching strain caused cardiac hypertrophy by increasing sarcomeric growth [10]. These data suggest that mechanical

stretching plays important roles in physiology and pathophysiology.

A previous study indicated that mechanical stretch induced a cardiac hypertrophic gene program in rat ventricular myocyte cells [11]. Here, we comprehensively characterized the time course of mechanical stretch-activated gene expression in a human cardiomyocyte cell line using a dynamic culture system. We also identified pathways enriched in genes that were differentially expressed after cyclic stretching. Finally, we confirmed NGS expression results for four genes associated with cholesterol biosynthesis and inflammatory response in an RT-PCR experiment.

RESULTS

Cyclic stretching alters gene expression profiles

Mechanical stimulation influences cell orientation, which consequently affects cell growth, differentiation, and many cellular functions. The effect of cyclic stretching on gene transcription was determined by

stretching AC16 human cardiomyocyte cells by 15% at a frequency of 0.5 Hz for 1, 4, 12, 24, and 48 hours. Among the differentially expressed genes identified in the 1, 4, and 12 hour stretching groups, relatively few that changed at least 2-fold in expression were shared by all three groups (Supplementary Table 2).

In contrast, a larger number of genes showing a 2-fold or greater change in expression were shared by both the 24 and 48 hour stretching groups (Figure 1). Expression of the Serpin Family E Member 1 (SERPINE1) gene, which encodes plasminogen activator inhibitor 1 (PAI-1) and is involved in blood clotting, was significantly increased at all the time points. SERPINE1 activity is especially crucial in injuries in which inhibition of fibrinolysis is necessary to protect the body from excessive blood loss.

Short- and long-term cyclic stretching differentially alter gene expression profiles

Clustering and principal component analysis are useful techniques for analyzing gene expression data that

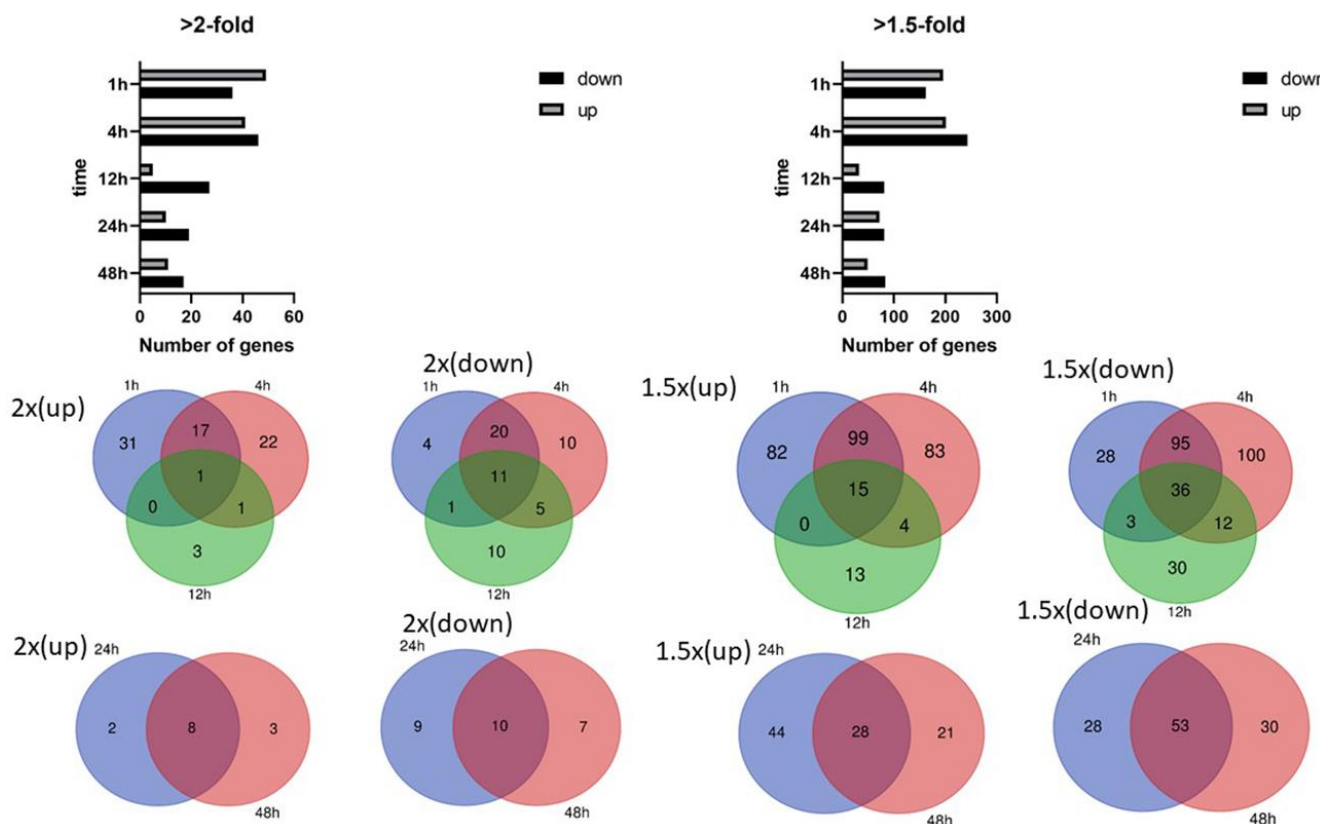


Figure 1. Differentially expressed genes in human cardiomyocytes. Numbers of differentially expressed genes after cyclic stretching: (A) Genes showing an at least 2-fold difference in expression; (B) genes showing an at least 1.5-fold difference in expression. Venn diagrams show the overlapping genes with at least 2-fold and 1.5-fold differences in expression.

involve many complex biological networks. Principal component analysis revealed that cells could be separated into groups based on the duration of cyclic mechanical stretching treatment. As shown in Figure 2, principal component analysis revealed that human cardiomyocytes could be separated into long-term (12, 24, and 48 hours) and short-term (1 and 4 hours) stretch effect groups. Gene expression profiles of cells treated with cyclic stretching for 1 and 4 hours had similar metrics which differed from those observed in the static condition (zero hour) group, which was not subjected to any cyclic mechanical stretching treatment (Figure 2).

Functional and pathway analysis of differentially expressed genes

Genes showing cyclic stretching-dependent differential expression (at least 2-fold difference) were further examined in a functional enrichment analysis using Ingenuity Pathway Analysis for diseases and biological functions. As shown in Figure 3, cyclic stretching-associated genes were enriched in organismal injury and

abnormalities ($p = 1.92E-29$), cardiovascular system development and function ($p = 1.36E-20$), and cellular movement ($p = 6.61E-20$). Cardiovascular system development and function included the development of vasculature, migration, neovascularization, and vascularization (Figure 3). Among the biological pathways, lipid metabolism was enriched in the 1-, 4-, and 12-hour cyclic stretching treatment groups. Genes that were differentially expressed response to 24 and 48 hours of cyclic stretching were enriched in tissue fibrosis and the inflammation pathway. The top five most significantly altered biological pathways at each time point are shown in Figure 4. Twenty-nine cyclic stretching-associated genes that were significantly differentially expressed in at least three of the time point groups are shown in the heatmap in Figure 5.

Validation of cyclic stretching-associated gene expression by real-time PCR

Short-term stretching for 1, 4, and 12 h significantly altered expression of genes associated with cholesterol biosynthesis, while long-term stretching for 24 and 48 h

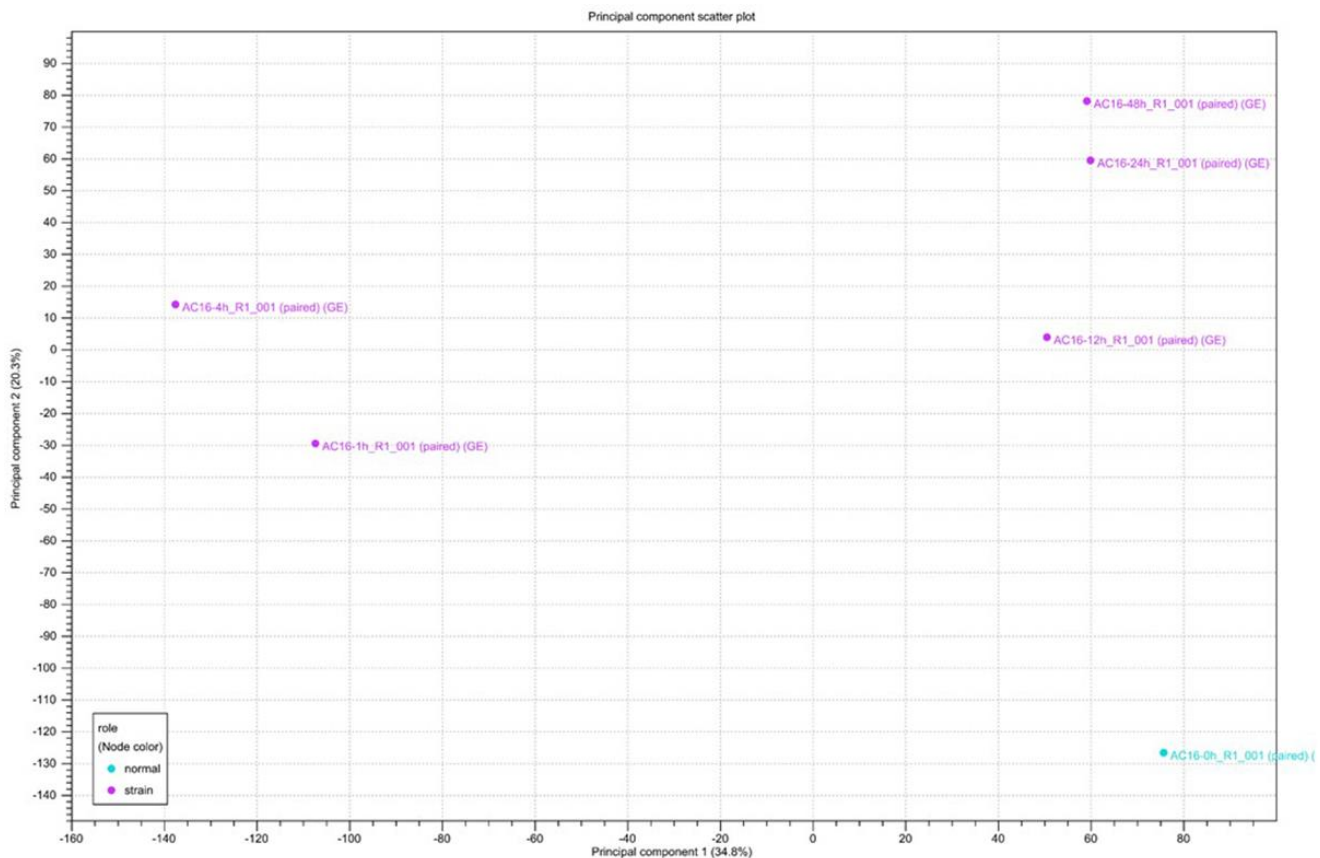


Figure 2. Principal component analysis (PCA) of RNA-seq data. Gene expression changes were investigated after 0, 1, 4, 12, 24, and 48 hours of cyclic stretching. PCA was performed using normalized RNA-Seq data for genes differentially expressed in one pairwise comparison: 0 h vs. other time points.

primarily affected expression of genes related to cell migration and enzymatic activity (Figure 4); other genes for which expression was altered by cyclic stretching are shown in Figure 5. Differentially expressed genes for which treatment effects differed between the short-term and long-term stretching groups are shown in

Supplementary Table 3. Among them, ID1 (short-term stretching effect), ID3 (short-term stretching effect), SERPINE1 (long-term stretching effect), and CCL2 (long-term stretching effect) were selected for qPCR validation. The amount of strain used was relevant to cardiac arrhythmia; acute arrhythmia affects cholesterol

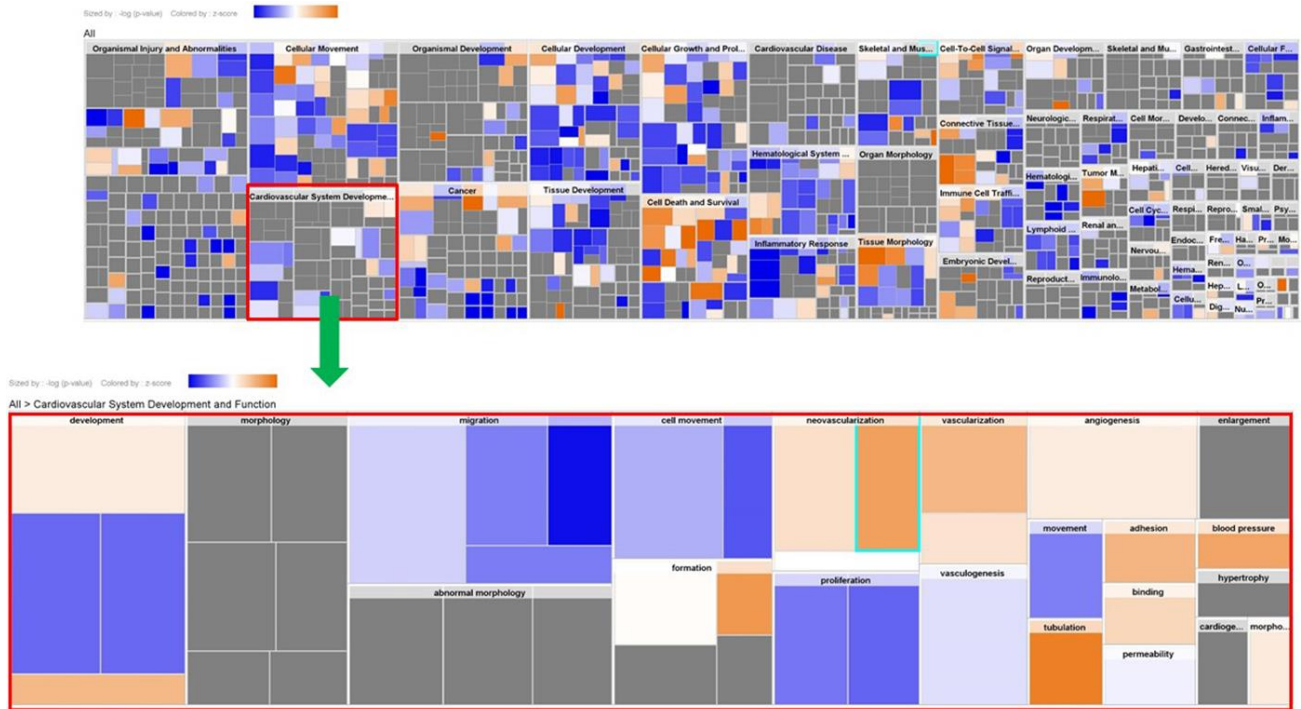


Figure 3. Expression analysis heatmap for disease and functional pathways.

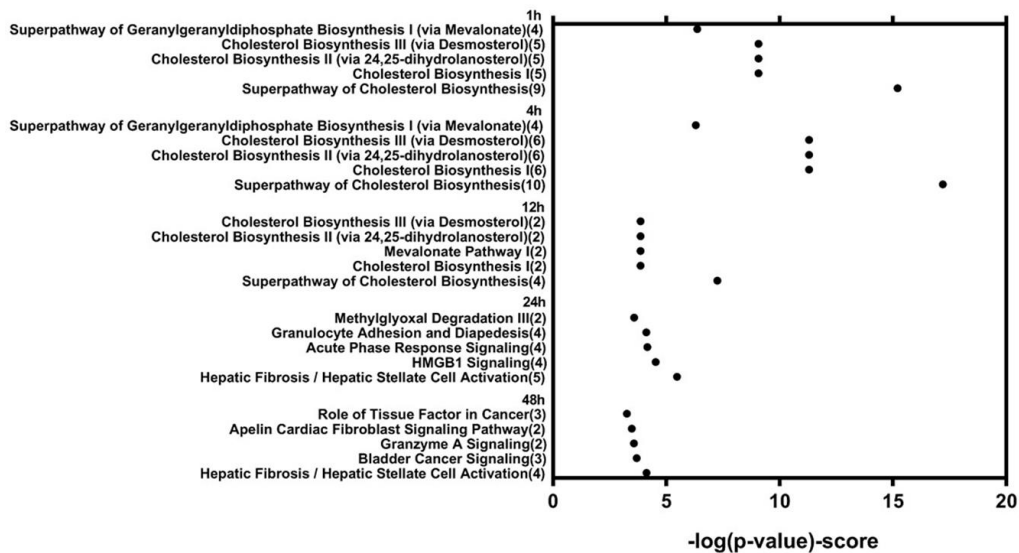


Figure 4. Functional analysis of differentially expressed genes in human cardiomyocytes after 1, 4, 12, 24, and 48 hours of cyclic stretching.

biosynthesis and metabolism, while prolonged arrhythmia decreases cell viability and activates various cellular signaling pathways. We found that ID1 expression increased significantly after 1 h of stretching, while ID3 expression increased significantly after 1, 4, 12, 24, and 48 h of stretching (Figure 6). CCL2, which is involved in injury-associated inflammatory processes in cardiac cells, decreased after all durations of cyclic stretching treatment (Figure 6).

DISCUSSION

Bone morphogenetic protein (BMP) signaling is involved in cyclic stretch-induced aortic valve calcification. Overproduction of BMP4 is pro-inflammatory in vascular cells and has been linked to hypertension [12, 13] and increases ID1 expression. ID1 expression is regulated by methylated cholesterol myristate, which has been linked to mesenchymal stem

cells (MSCs) and neuronal cell survival [14, 15]. In addition, cyclic stretching is involved in the induction of lipotoxicity during atrial myocyte enlargement [16]. Together, these findings suggest that cyclic stretching greatly impacts the BMP4 signaling-dependent cholesterol biosynthesis pathway. Although it is acknowledged that disturbances in cholesterol biosynthesis may lead to cardiac disease [17], the effects of mechanical stretch on cholesterol biosynthesis remain unclear.

The ID1 gene, which encodes DNA-binding protein inhibitor ID-1, is an early downstream target of BMP4 signaling in various cells, including endothelial cells and embryonic stem cells [15, 18]. For example, ID1 is activated by Activin A receptor-like Type 1 (ALK1), which is a target gene of BMP [12]. Furthermore, ID1 activity during BMP receptor II (BMPRII) transition in lipid rafts may lead to abnormal cell growth [19].

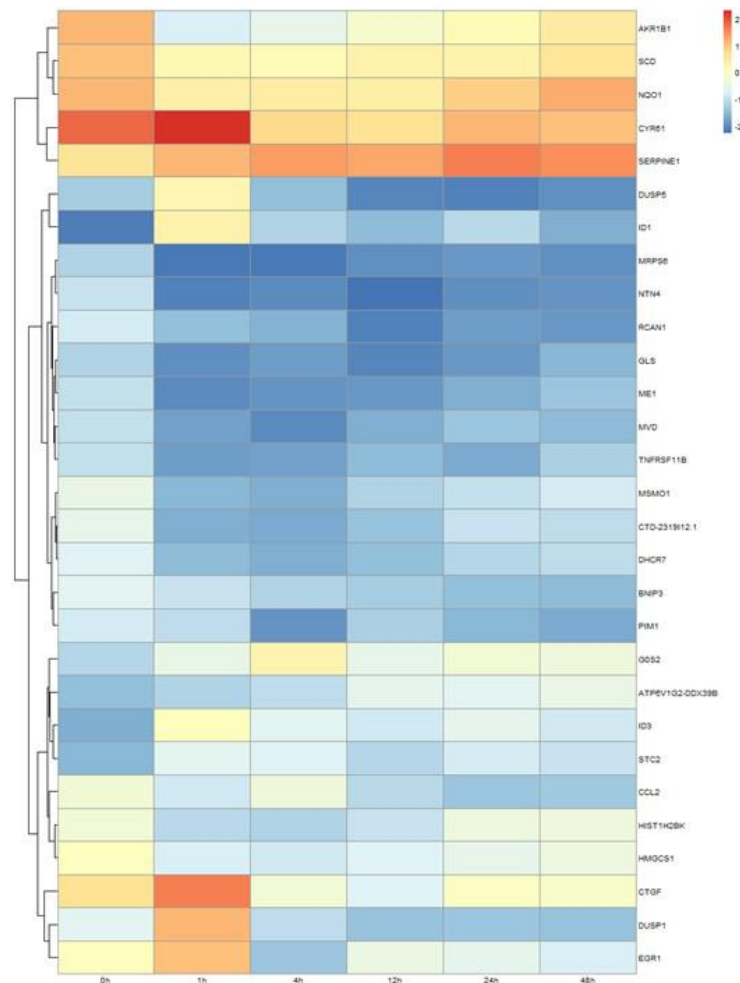


Figure 5. Differential expression profile of 29 genes after 1, 4, 12, 24, and 48 hours of cyclical stretching in human cardiomyocytes. The heat map diagram shows expression changes for 29 genes that were altered in cardiac myocytes in response to at least three time points of mechanical stretching.

However, whether ID gene expression is affected by mechanical stretch remains unclear. In this study, we found that cyclic stretching was associated with changes in the cholesterol biosynthesis signaling pathway. Specifically, ID1 gene expression increased after one hour of cyclic stretching. Furthermore, increases in expression of the SERPINE1 and ID3 genes, which are associated with obesity, and a decrease in pro-inflammatory CCL2 gene expression highlighted the impact of mechanical stretch on the cholesterol biosynthesis pathway.

Because ID1 plays roles in cell growth, differentiation, and apoptosis [20, 21], mechanical stretch might also affect these processes by altering its expression. Increases in CYR61 gene expression, which affects cell adhesion and proliferation, after one hour of stretching indicate that it may impact those processes as well. Such increases in anti-apoptotic and pro-survival genes at early time points may help maintain various cellular functions and signaling mechanisms. In contrast, after 24 and 48 hours of mechanical stretching, gene expression increases shifted from the cholesterol biosynthesis pathway to disease pathways, including acute phase response, cancer signaling, and hepatic fibrosis. Furthermore, no significant differences in genes showing differential expression were observed between the 24- and 48-hour mechanical stretching

groups, indicating that 24 hours of stretching induced a relatively stable pro-inflammatory response that followed changes to the cholesterol-signaling pathway.

In this study, we examined transcriptional profile changes in human cardiomyocytes in response to cyclic stretching for the first time. Expression of a gene that has been previously linked to BMP signaling was altered after one hour of short-term cyclic stretching. BMPs exert both paracrine and autocrine effects and can also bind to type 1 or type 2 receptors to trigger intracellular signaling [22]. Endothelial cells, fibroblasts, and vascular smooth muscle cells express BMP2 and BMP4, which are important for heart development in vertebrates [23, 24]. Increases in BMP4 expression are associated with increased cholesterol levels, and BMP4 targets the ID1 promoter to drive anti-apoptotic cellular activities [25, 26]. Cholesterol myristate mediates ID1 activity, which promotes activation of B-cell lymphoma-extra large (Bcl-xL), leading to inhibition of cytochrome c release from mitochondria and decreased caspase activity [15]. In order to effectively promote survival, this BMP4-ID1 signaling cascade must be activated before the pro-inflammatory response is activated. The balance between cholesterol-mediated survival and pro-inflammatory responses can therefore determine whether normal or disease states are maintained.

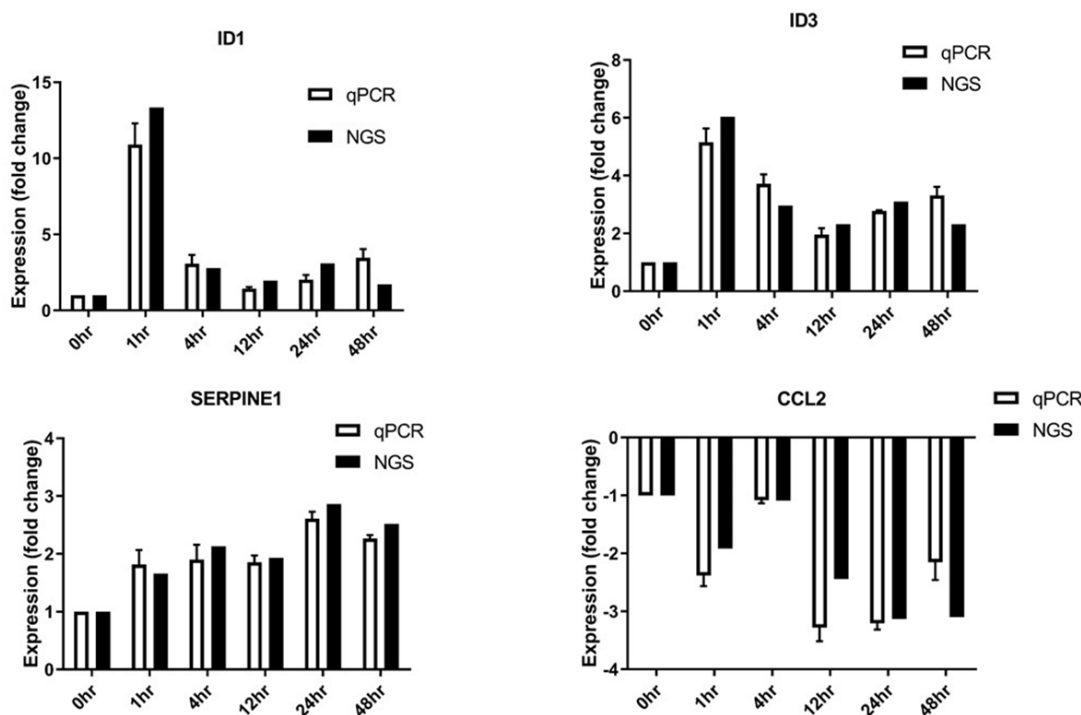


Figure 6. Differentially expressed genes validated by RT-qPCR. SERPINE1, ID1, ID3, and CCL2 mRNA levels were analyzed (n = 3 in all groups).

While we examined the effects of mechanical load in cardiomyocytes, it also affects other cell types, including vascular, neuronal and bone cells, *in vivo* [27–30]. Our results highlight the crucial effects mechanical stretching can have on the cholesterol biosynthesis pathway as well as in cardiac disease. Furthermore, prolonged stretching could be a key cause of cardiomyopathy and various cardiovascular diseases. A better understanding of cholesterol metabolism could provide additional insights into the effects of mechanical stretching and the prevention of cardiac diseases in general.

Some limitations should be considered when interpreting the results of this study. Although the human cardiomyocyte cell line we used to examine the effects of cyclic stretching reflects human cardiac physiology relatively well, the cells will eventually undergo spontaneous differentiation and lose their morphology after long-term culture. In addition, they do not undergo spontaneous contraction or relaxation. However, since they can be serially passaged *in vitro* and further differentiated when cultured under mitogen-free conditions, human cardiomyocytes are ideal for developmental and pathological studies [31, 32]. Nevertheless, the results in this study pertain to proliferating cardiomyocytes, and additional studies will be necessary to determine their relevance to other types of cardiac cells.

In conclusion, in this study we describe expression profiles for genes that are differentially expressed in response to cyclic stretching in cardiomyocytes. Furthermore, we confirmed alterations in ID1 and SERPINE mRNA levels, which are likely involved in the cholesterol biosynthesis pathway. These results may improve our understanding of the cellular signaling pathways underlying cardiac injury.

MATERIALS AND METHODS

Cyclic stretching

Human ventricular cardiomyocyte cells (AC16) were maintained in DMEM/F12 (GeneDireX Incorporation, Taiwan) supplemented with 10% fetal bovine serum (Fisher Scientific, Pittsburgh, PA, USA), 100 IU/mL penicillin (Sigma-Aldrich) and 100 µg/mL streptomycin (Sigma-Aldrich). Cells were incubated in a humidified atmosphere at 37°C with 5% CO₂. The cells were passaged every 3 to 4 days, and passages 2 to 10 were used in this study.

Stretching device

The cells were stretched using a stretching device from ARTEMIS ATMS Boxer (TAIHOYA Corporation,

Kaohsiung, Taiwan). Cells were seeded on polydimethylsiloxane (PDMS) pre-coated with collagen type 1 overnight. The next day, cells were stretched at 15% strain and a frequency of 0.5 Hz for at 0, 1, 4, 12, 24, or 48 h.

RNA isolation

Total RNA was isolated using Trizol (Invitrogen) according to the manufacturer's instructions. Briefly, chloroform was added to the mixture, followed by thorough mixing and centrifugation at 12,000 G for 15 min at 4°C. The clear supernatant was collected in a new microtube and isopropanol was added, followed by thorough mixing and centrifugation at 12,000 G for 15 min at 4°C. Finally, the RNA was washed with 75% ethanol and centrifuged at 7000 G for 5 min at 4°C. The RNA pellet was air-dried, reconstituted in DEPC water, and stored at -80°C.

RNA sequencing

RNA sample quality was assessed using a NanoDrop spectrophotometer (Thermo Fisher Scientific Inc.) and a Bioanalyzer 2100 (Agilent Technologies, Santa Clara, CA, USA). The total RNA was subjected to NGS library construction using the MGIEasy RNA Library Prep Set (MGI Tech Co., Ltd., China). The quality and the average length of the sequence library for each sample were assessed using either the Bioanalyzer (Agilent Technologies, Santa Clara, CA, USA) or the DNA 1000 kit. The indexed samples were pooled equimolarly and sequenced on the BGISEQ-500 platform (50 bases, single-end reads) (BGI, China). The RNAseq data are publicly available on NCBI's Sequence Read Archive (SRA) database. (Bio-project: PRJNA612764).

Sequencing data analysis

Clean reads were generated from raw sequencing reads, which were filtered to remove the adapters, unknown biases, and low quality reads. Clean reads were aligned to the reference genome build using Bowtie2 v2.2.5 [33]. For gene expression analysis, the matched reads were calculated and then normalized to FPKM using RSEM [34]. PCA analysis was performed with all samples using CLC Genomics Workbench (QIAGEN company, Redwood City, CA, USA), and diagrams were drawn with ggplot2 with functions of R. The gene expression data are listed in Supplementary Table 1.

Functional enrichment analysis

Pathway enrichment was analyzed using Ingenuity Pathway Analysis (IPA) (QIAGEN company, Redwood

City, CA, USA). The core analysis was based on a 2-fold change minimum in the gene profile. Significant pathways ($p < .05$) were identified using the database.

Real-time PCR (RT-qPCR)

The differentially expressed genes identified by RNAseq were confirmed by performing quantitative real-time polymerase chain reaction (RT-qPCR) for four selected genes – ID1, ID3, CCL2, and SERPINE1. First, first-strand cDNA was generated from 0.1 µg of RNA using a ProtoScript® II First Strand cDNA Synthesis Kit (New England Biolabs, Inc., USA) in the presence of oligo-dT primers. After cDNA amplification, qPCR reactions were run on an ABI™ StepOne™ Real-Time PCR System (Applied Biosystems, Foster City, CA, USA) with KAPA SYBR® FAST Master Mix (2X) ABI Prism™ (KAPA BIOSYSTEMS, Boston, Massachusetts, United States). Gene expression levels were normalized to the expression of the internal housekeeping gene GAPDH. Relative quantification was calculated using the 2^{-ΔΔCT} method. The sequences of the primers used are listed in Supplementary Table 1.

AUTHOR CONTRIBUTIONS

CC C., CY K., and YC H. made substantial contributions to conception and design. YC H. and TY W. wrote the manuscript. TY C. and WH L. interpreted and analyzed the data with CY K. and YH C. All authors approved the final manuscript.

CONFLICTS OF INTEREST

All authors of this manuscript have no conflicts of interest to declare.

FUNDING

This study was supported by grants from Show Chwan and Chan Bing Show Chwan Memorial Hospital (RD107053) and the Ministry of Science and Technology (MOST 107-2314-B-008-002).

REFERENCES

- Schwartz L, da Veiga Moreira J, Jolicoeur M. Physical forces modulate cell differentiation and proliferation processes. *J Cell Mol Med.* 2018; 22:738–45. <https://doi.org/10.1111/jcmm.13417> PMID:29193856
- Jufri NF, Mohamedali A, Avolio A, Baker MS. Mechanical stretch: physiological and pathological implications for human vascular endothelial cells. *Vasc Cell.* 2015; 7:8. <https://doi.org/10.1186/s13221-015-0033-z> PMID:26388991
- MacQueen L, Sun Y, Simmons CA. Mesenchymal stem cell mechanobiology and emerging experimental platforms. *J R Soc Interface.* 2013; 10:20130179. <https://doi.org/10.1098/rsif.2013.0179> PMID:23635493
- Fu X, Liu G, Halim A, Ju Y, Luo Q, Song AG. Mesenchymal stem cell migration and tissue repair. *Cells.* 2019; 8:784. <https://doi.org/10.3390/cells8080784> PMID:31357692
- Fang B, Liu Y, Zheng D, Shan S, Wang C, Gao Y, Wang J, Xie Y, Zhang Y, Li Q. The effects of mechanical stretch on the biological characteristics of human adipose-derived stem cells. *J Cell Mol Med.* 2019; 23:4244–55. <https://doi.org/10.1111/jcmm.14314> PMID:31020802
- Dasgupta I, McCollum D. Control of cellular responses to mechanical cues through YAP/TAZ regulation. *J Biol Chem.* 2019; 294:17693–706. <https://doi.org/10.1074/jbc.REV119.007963> PMID:31594864
- Machiraju P, Greenway SC. Current methods for the maturation of induced pluripotent stem cell-derived cardiomyocytes. *World J Stem Cells.* 2019; 11:33–43. <https://doi.org/10.4252/wjsc.v11.i1.33> PMID:30705713
- Mihic A, Li J, Miyagi Y, Gagliardi M, Li SH, Zu J, Weisel RD, Keller G, Li RK. The effect of cyclic stretch on maturation and 3D tissue formation of human embryonic stem cell-derived cardiomyocytes. *Biomaterials.* 2014; 35:2798–808. <https://doi.org/10.1016/j.biomaterials.2013.12.052> PMID:24424206
- Besser RR, Ishahak M, Mayo V, Carbonero D, Claire I, Agarwal A. Engineered microenvironments for maturation of stem cell derived cardiac myocytes. *Theranostics.* 2018; 8:124–40. <https://doi.org/10.7150/thno.19441> PMID:29290797
- Yang H, Schmidt LP, Wang Z, Yang X, Shao Y, Borg TK, Markwald R, Runyan R, Gao BZ. Dynamic myofibrillar remodeling in live cardiomyocytes under static stretch. *Sci Rep.* 2016; 6:20674. <https://doi.org/10.1038/srep20674> PMID:26861590
- Rysä J, Tokola H, Ruskoaho H. Mechanical stretch induced transcriptomic profiles in cardiac myocytes. *Sci Rep.* 2018; 8:4733. <https://doi.org/10.1038/s41598-018-23042-w> PMID:29549296

12. Luo JY, Zhang Y, Wang L, Huang Y. Regulators and effectors of bone morphogenetic protein signalling in the cardiovascular system. *J Physiol.* 2015; 593:2995–3011.
<https://doi.org/10.1113/JP270207>
PMID:[25952563](https://pubmed.ncbi.nlm.nih.gov/25952563/)
13. Wong WT, Tian XY, Chen Y, Leung FP, Liu L, Lee HK, Ng CF, Xu A, Yao X, Vanhoutte PM, Tipoe GL, Huang Y. Bone morphogenetic protein-4 impairs endothelial function through oxidative stress-dependent cyclooxygenase-2 upregulation: implications on hypertension. *Circ Res.* 2010; 107:984–91.
<https://doi.org/10.1161/CIRCRESAHA.110.222794>
PMID:[20724703](https://pubmed.ncbi.nlm.nih.gov/20724703/)
14. Chen DF, Zhang HL, Du SH, Li H, Zhou JH, Li YW, Zeng HP, Hua ZC. Cholesterol myristate suppresses the apoptosis of mesenchymal stem cells via upregulation of inhibitor of differentiation. *Steroids.* 2010; 75:1119–26.
<https://doi.org/10.1016/j.steroids.2010.07.009>
PMID:[20674581](https://pubmed.ncbi.nlm.nih.gov/20674581/)
15. Chen DF, Cao JH, Liu Y, Wu Y, Du SH, Li H, Zhou JH, Li YW, Zeng HP, Hua ZC. BMP-id pathway targeted by cholesterol myristate suppresses the apoptosis of PC12 cells. *Brain Res.* 2011; 1367:33–42.
<https://doi.org/10.1016/j.brainres.2010.10.025>
PMID:[20970407](https://pubmed.ncbi.nlm.nih.gov/20970407/)
16. Fang CY, Chen MC, Chang TH, Wu CC, Chang JP, Huang HD, Ho WC, Wang YZ, Pan KL, Lin YS, Huang YK, Chen CJ, Lee WC. Id1 and Hmgs2 are affected by stretch in HL-1 atrial myocytes. *Int J Mol Sci.* 2018; 19:4094.
<https://doi.org/10.3390/ijms19124094>
PMID:[30567295](https://pubmed.ncbi.nlm.nih.gov/30567295/)
17. Daniels TF, Killinger KM, Michal JJ, Wright RW Jr, Jiang Z. Lipoproteins, cholesterol homeostasis and cardiac health. *Int J Biol Sci.* 2009; 5:474–88.
<https://doi.org/10.7150/ijbs.5.474>
PMID:[19584955](https://pubmed.ncbi.nlm.nih.gov/19584955/)
18. Fei T, Xia K, Li Z, Zhou B, Zhu S, Chen H, Zhang J, Chen Z, Xiao H, Han JD, Chen YG. Genome-wide mapping of SMAD target genes reveals the role of BMP signaling in embryonic stem cell fate determination. *Genome Res.* 2010; 20:36–44.
<https://doi.org/10.1101/gr.092114.109>
PMID:[19926752](https://pubmed.ncbi.nlm.nih.gov/19926752/)
19. Mundy C, Yang E, Takano H, Billings PC, Pacifici M. Heparan sulfate antagonism alters bone morphogenetic protein signaling and receptor dynamics, suggesting a mechanism in hereditary multiple exostoses. *J Biol Chem.* 2018; 293:7703–16.
<https://doi.org/10.1074/jbc.RA117.000264>
PMID:[29622677](https://pubmed.ncbi.nlm.nih.gov/29622677/)
20. Norton JD, Atherton GT. Coupling of cell growth control and apoptosis functions of id proteins. *Mol Cell Biol.* 1998; 18:2371–81.
<https://doi.org/10.1128/mcb.18.4.2371>
PMID:[9528806](https://pubmed.ncbi.nlm.nih.gov/9528806/)
21. Zhao Y, Luo A, Li S, Zhang W, Chen H, Li Y, Ding F, Huang F, Liu Z. Inhibitor of differentiation/DNA binding 1 (ID1) inhibits etoposide-induced apoptosis in a c-jun/c-fos-dependent manner. *J Biol Chem.* 2016; 291:6831–42.
<https://doi.org/10.1074/jbc.M115.704361>
PMID:[26858249](https://pubmed.ncbi.nlm.nih.gov/26858249/)
22. Morrell NW, Bloch DB, ten Dijke P, Goumans MJ, Hata A, Smith J, Yu PB, Bloch KD. Targeting BMP signalling in cardiovascular disease and anaemia. *Nat Rev Cardiol.* 2016; 13:106–20.
<https://doi.org/10.1038/nrcardio.2015.156>
PMID:[26461965](https://pubmed.ncbi.nlm.nih.gov/26461965/)
23. Balligand JL, Feron O, Dessy C. eNOS activation by physical forces: from short-term regulation of contraction to chronic remodeling of cardiovascular tissues. *Physiol Rev.* 2009; 89:481–534.
<https://doi.org/10.1152/physrev.00042.2007>
PMID:[19342613](https://pubmed.ncbi.nlm.nih.gov/19342613/)
24. Segers VF, Brutsaert DL, De Keulenaer GW. Cardiac remodeling: endothelial cells have more to say than just NO. *Front Physiol.* 2018; 9:382.
<https://doi.org/10.3389/fphys.2018.00382>
PMID:[29695980](https://pubmed.ncbi.nlm.nih.gov/29695980/)
25. Feng J, Gao J, Li Y, Yang Y, Dang L, Ye Y, Deng J, Li A. BMP4 enhances foam cell formation by BMPR-2/Smad1/5/8 signaling. *Int J Mol Sci.* 2014; 15:5536–52.
<https://doi.org/10.3390/ijms15045536>
PMID:[24690996](https://pubmed.ncbi.nlm.nih.gov/24690996/)
26. Lewis TC, Prywes R. Serum regulation of Id1 expression by a BMP pathway and BMP responsive element. *Biochim Biophys Acta.* 2013; 1829:1147–59.
<https://doi.org/10.1016/j.bbagr.2013.08.002>
PMID:[23948603](https://pubmed.ncbi.nlm.nih.gov/23948603/)
27. Arulmoli J, Pathak MM, McDonnell LP, Nourse JL, Tombola F, Earthman JC, Flanagan LA. Static stretch affects neural stem cell differentiation in an extracellular matrix-dependent manner. *Sci Rep.* 2015; 5:8499.
<https://doi.org/10.1038/srep08499> PMID:[25686615](https://pubmed.ncbi.nlm.nih.gov/25686615/)
28. Riehl BD, Park JH, Kwon IK, Lim JY. Mechanical stretching for tissue engineering: two-dimensional and three-dimensional constructs. *Tissue Eng Part B Rev.* 2012; 18:288–300.
<https://doi.org/10.1089/ten.TEB.2011.0465>
PMID:[22335794](https://pubmed.ncbi.nlm.nih.gov/22335794/)

29. Tulloch NL, Muskheli V, Razumova MV, Korte FS, Regnier M, Hauch KD, Pabon L, Reinecke H, Murry CE. Growth of engineered human myocardium with mechanical loading and vascular coculture. *Circ Res*. 2011; 109:47–59.
<https://doi.org/10.1161/CIRCRESAHA.110.237206>
PMID:[21597009](https://pubmed.ncbi.nlm.nih.gov/21597009/)
30. Potter CM, Lao KH, Zeng L, Xu Q. Role of biomechanical forces in stem cell vascular lineage differentiation. *Arterioscler Thromb Vasc Biol*. 2014; 34:2184–90.
<https://doi.org/10.1161/ATVBAHA.114.303423>
PMID:[25012135](https://pubmed.ncbi.nlm.nih.gov/25012135/)
31. Davidson MM, Nesti C, Palenzuela L, Walker WF, Hernandez E, Protas L, Hirano M, Isaac ND. Novel cell lines derived from adult human ventricular cardiomyocytes. *J Mol Cell Cardiol*. 2005; 39:133–47.
<https://doi.org/10.1016/j.yjmcc.2005.03.003>
PMID:[15913645](https://pubmed.ncbi.nlm.nih.gov/15913645/)
32. Litzkas P, Jha KK, Ozer HL. Efficient transfer of cloned DNA into human diploid cells: protoplast fusion in suspension. *Mol Cell Biol*. 1984; 4:2549–52.
<https://doi.org/10.1128/mcb.4.11.2549>
PMID:[6096698](https://pubmed.ncbi.nlm.nih.gov/6096698/)
33. Langmead B, Salzberg SL. Fast gapped-read alignment with bowtie 2. *Nat Methods*. 2012; 9:357–59.
<https://doi.org/10.1038/nmeth.1923>
PMID:[22388286](https://pubmed.ncbi.nlm.nih.gov/22388286/)
34. Li B, Dewey CN. RSEM: accurate transcript quantification from RNA-seq data with or without a reference genome. *BMC Bioinformatics*. 2011; 12:323.
<https://doi.org/10.1186/1471-2105-12-323>
PMID:[21816040](https://pubmed.ncbi.nlm.nih.gov/21816040/)

SUPPLEMENTARY MATERIALS

Supplementary Tables

Supplementary Table 1. List of primer sequences used for real time PCR analysis in this study.

Gene name	sequence (5'- 3')
ID1-F	GTAAACGTGCTGCTCTACGACATGA
ID1-R	AGCTCCAAGTGAAGGTCCCTGA
ID3-F	TCATCTCCAACGACAAAAGG
ID3-R	ACCAGGTTTAGTCTCCAGGAA
GAPDH-F	TGCACCACCAACTGCTTAGC
GAPDH-R	GGCATGGACTGTGGTCATGAG
CCL2-F	GCTCATAGCAGCCACCTTCATTC
CCL2-R	GGACACTTGCTGCTGGTGATTC
SERPINE1-F	CACAAATCAGACGGCAGCACT
SERPINE1-R	CATCGGGCGTGGTGAATC

F: Forward primer. R: reverse primer.

Please browse Full Text version to see the data of Supplementary Tables 2

Supplementary Table 2. The gene expression profile with a 2-fold significance at each time point.

Supplementary Table 3. The consistency DEG gene list in the short-term and long term stretch effect in the human cardiomyocytes.

Short term	Long term
AKR1B1	AKR1B1
COL6A3	ATP6V1G2-DDX39B
CTD-2319I12.1	BNIP3
DDX21	CCL2
DHCR7	CTGF
ERRFI1	CYR61
F3	DUSP1
FOSL1	DUSP5
HIST1H2BK	G0S2
HMGCS1	HMOX1
ID1	ID3
ID3	MMP14
IL11	MMP2
MAFF	NTN4
MAFK	PIM1
ME1	RCAN1
MOK	SEMA7A
MRPS6	SERPINE1
MSMO1	
MVD	
NQO1	
ODC1	
RBM3	
RRS1	
SCD	
SDC4	
SERPINB2	
STC2	
TAGLN	
TM4SF1	